



ARTICLE

Bio-Adhesives Combined with Lotus Leaf Fiber to Prepare Bio-Composites for Substituting the Plastic Packaging Materials

Ke Shi^{1,2}, Luyang Wang^{1,2}, Ruige Qi^{1,2} and Chunxia He^{1,2,*}

¹College of Engineering, Nanjing Agricultural University, Nanjing, 210031, China

²Key Laboratory of Intelligent Agricultural Equipment in Jiangsu Province, Nanjing, 210031, China

*Corresponding Author: Chunxia He. Email: chunxiahenjau@163.com

Received: 15 June 2021 Accepted: 22 August 2021

ABSTRACT

This work was aim to prepare a packing material from natural resources to reduce the environment pollution caused by plastics. Four bio-adhesives (guar gum, sodium alginate, agar and chitosan) were combined with lotus leaf fibers to prepare degradable composites, respectively. The mechanical properties, moisture absorption profiles and the thermal conductivity of the composites were studied and the cross section morphology and the thermal properties of the composites were analyzed. The Fourier-transform infrared spectroscopy (FTIR) results showed that the polar groups such as $-OH$ and $-COO^-$ in bio-adhesives can form hydrogen bond with $-OH$ in lotus leaf fibers to connect the two components. The combination of agar and lotus leaf fiber was good, and their composite had the best mechanical properties, with the tensile strength, flexural strength and impact strength of 2.05, 5.9 MPa and $4.29 \text{ kJ}\cdot\text{m}^{-2}$, respectively, and the composite had a low moisture absorption profile, and the equilibrium moisture absorption rate was 32.32%. The lotus leaf fiber/agar composite (LAC) had an excellent comprehensive performance and it was non-toxic, degradable and thermal insulating, which indicated that it had the potential to use in packaging field to substitute plastics.

KEYWORDS

Bio-adhesive; lotus leaf fiber; composite; mechanical properties; morphology

1 Introduction

Plastic brings convenience to human life, while its non-degradable characteristics make it spread all over the world along with the food chain and atmospheric circulation. At present, some researchers found the existence of micro plastic in the snow of Mount Everest [1]. The micro and nano size plastics were reported in the food of human life, such as vegetables [2], seafood [3], rice [4], drinking water [5], milk [6], etc. Plastic pollution is an urgent problem in the world and countries and regions all over the world have successively issued a series of relevant policies and measures to control or prohibit plastics [7–11]. Since the Chinese government prohibited the production and sale of disposable plastic tableware in 2020, the catering industry is looking for suitable substitutes. At present, paper tableware is widely used in the market, but it is easy to absorb water, deform and lose its efficacy, so it is necessary to develop a new type of eco-friendly material to meet the demand.



Bio-composites are made of natural materials with the character of degradability and can be given way to be economically viable substitutes for disposable plastics. Li et al. [12] studied the composite film made of cellulose nanofiber (CNF) and corn starch from sweet cabbage leaves, and found that the addition of CNF can significantly improve the hydrophobicity of the composite film. Ramesh et al. [13] studied the properties of the composite prepared by cellulose nanoparticles (CNP), fennel seed oil and polyvinyl alcohol (PVA), and found that the composite is degradable and has good antibacterial and antioxidant properties, which can be used for food packaging. Ortega-Toro et al. [14] prepared bio-composites made of corn starch and polycaprolactone (PCL). The composites had no toxic compounds and had good food compatibility, which could be used in food packaging to replace disposable plastics. With the shortage of petroleum resources, the improvement of national laws and regulations and the enhancement of people's environmental awareness, the research on the preparation of green adhesives from biomass resources and their derivatives have attracted the attention of many scholars. Li et al. [15] prepared the wheat straw fiber reinforced starch composite, and found that when the ratio of fiber and starch was 2:5, the compressive strength of the composite was the best, which could be used to replace EPS, EPE and other plastic packaging materials. Jancikova et al. [16] prepared a biodegradable composite membrane by using the hydrolysate of gelatin, red algal glue, and dry leaves. The dry leaves were found to improve the oxidation resistance, such a composite can be used to package food. Tongdeesoontorn et al. [17] studied the effects of different oxidants on the properties of cassava starch/gelatin film, and found that the cassava starch/gelatin film containing quercetin and tert butyl hydroquinone (TBHQ) can retard the oxidation of lard, and this film can be used as an active packaging material to delay the oxidation in food. Bio-adhesives are the ideal materials extracted from plants or animals, which are non-toxic and degradable. Guar gum is a highly purified natural polysaccharide with good biocompatibility and non-toxicity. It is often used as thickener and binder in food processing, chemical industry and other fields [18]. Sodium alginate, extracted from natural brown algae, is a kind of linear anionic polysaccharide, which is widely used in food and medical industry [19]. Agar is a completely degradable biomass material extracted from algae which is commonly used in food industry, biomedicine, biopharmaceutical and other fields [20]. Chitosan is an alkaline polysaccharide with good biocompatibility, bacteriostatic, blood coagulation, and degradability, it can be used in food, medicine, chemical industry, etc. [21].

Lotus leaf is a common natural resource and an ideal raw material for bio-composites as it is degradable and widely available. While, people's research on it mainly focuses on the special super hydrophobic structure on its surface, and there is little research on the application of it [22]. Some research have shown that biomass composites are easy to absorb moisture and deteriorate, and glycerol can be used as a waterproof agent to reduce its moisture absorption performance [23].

In order to reduce plastic pollution and expand the application of lotus leaf, in this paper, four kinds of bio-adhesives (guar gum, sodium alginate, agar and chitosan) and lotus leaf fiber were used to prepare bio-composites, respectively and glycerol was added as waterproof agent. The mechanical properties, moisture absorption profiles, thermal conductivity and cross section morphology of the composites were analyzed to explore the feasibility of the application in the field of food packaging.

2 Materials and Methods

2.1 Materials

Guar gum (food grade) was obtained from Beijing Guarrun Technology Company (Beijing, China), sodium alginate (food grade) was provided by Qingdao Mingyue Seaweed Group Company (Qingdao, China), agar (food grade) was the production of the Zhejiang Yinuo Biology Science and Technology Company (Zhejiang, China) and the Nanjing Ximeino Biotechnology Company (Nanjing, China) supplied the chitosan (food grade). The lotus leaf fibers were obtained from a farm in Bozhou in the Anhui Province of China. The hand-picked leaves were washed and cleaned with running water and

naturally dried at room temperature. The dried leaves were crushed and screened to 100 meshes to get the fibers. Glycerin was obtained from the Tianjin Zhiyuan Chemical Agent Company (Tianjin, China). The bio-adhesive samples and the process of lotus leaf fibers are shown in Fig. 1.

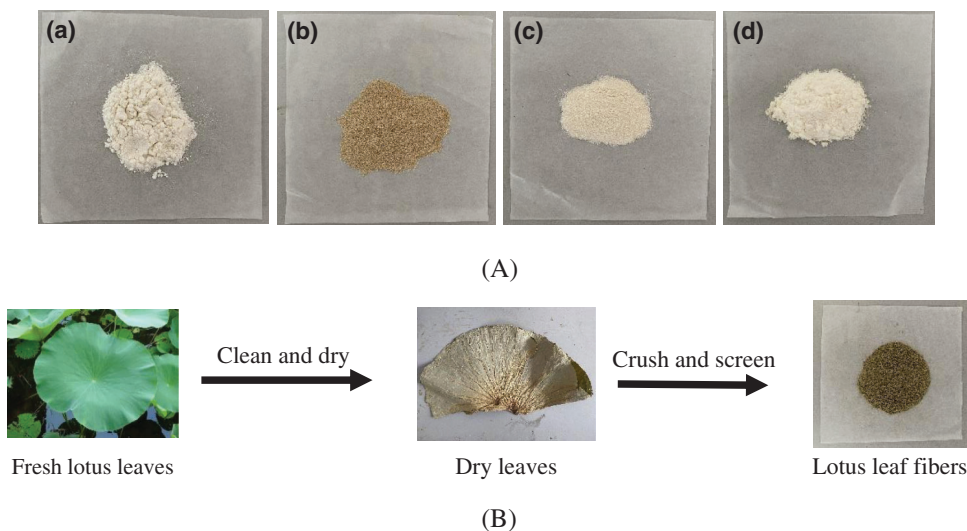


Figure 1: (A) The bio-adhesive samples of (a) Guar gum, (b) Sodium alginate, (c) Agar and (d) Chitosan, (B) The process of lotus leaf fibers

2.2 Preparation of Composites

The bio-adhesive and lotus leaf fiber and were evenly mixed, the bio-adhesive was 20% of the total mass, and 10% glycerol of the total mass was added. The mixture was well distributed in a 100 mm × 100 mm metal mold and then compressed at 120°C under 10 MPa of pressure for 30 min by using a XLB-D 400 × 400 × 2-Z flat vulcanizer (Shanghai Qicai Hydraulic Machinery Company, Shanghai, China). Finally, a 100 mm × 100 mm × 2 mm board was obtained. The lotus leaf fibers combined guar gum, sodium alginate, agar and chitosan composites were referred as LGC, LSC, LAC and LCC, respectively. The composite samples are shown in Fig. 2.



Figure 2: The composite samples made of LGC, LSC, LAC and LCC

2.3 Characterizations

2.3.1 Fourier-Transform Infrared Spectroscopy (FTIR)

The characteristic functional groups of fibers and agar were analyzed at room temperature by using a Nicolet iS-10 spectrometer (Thermo Fischer Scientific, Waltham, USA). Samples were grounded well with KBr (2% by weight) and pressed into a pellet with the thickness of about 1 mm. The

FTIR transmittance spectra were recorded after an average of 16 scans from 4,000 to 500 cm^{-1} and the resolution is 4 cm^{-1} .

2.3.2 Morphological Studies

The the tensile cross section images of composites were investigated using a Hitachi S-4800 scanning electron microscope (Tokyo, Japan). The cross section of the samples was sprayed with gold before scanning.

2.3.3 Mechanical Properties

The tensile strength and flexural strength properties were tested according to the GB/T standards 1040.1-2006 [24] and GB/T 9341-2008 [25], respectively. The tests were carried out by using a universal testing machine (CMT6104, Metz Industrial System (China) Co., Ltd., Shanghai, China), and the test rate was set at 2 $\text{mm}\cdot\text{min}^{-1}$. A XJJ-5 simply supported beam impact testing machine (Chengde Jinjian Testing Instrument Company, Chengde, China) was used to test the impact strength according to the GB/T 1043.1-2008 [26]. Each sample was tested three times to obtain the average value.

2.3.4 Thermogravimetric Analysis (TGA)

The thermal stability of composites was studied by using an STA 449 F3 Jupiter simultaneous thermal analyzer (NETZSCH, Selb, Germany). 10 mg of specimens were taken and the tests were carried out in argon atmosphere from 35°C to 800°C at a rate of 20 °C/min and a flow rate of 20 mL/min.

2.3.5 Moisture Absorption Performance

The moisture absorption rate was tested according to the GB/T standard 20312-2006 [27] in an HZ-2004G constant temperature and humidity box (Dongguan Hengzhun (Lixian) Instrument Scientific Company, Dongguan, China). The temperature was set to $(23 \pm 0.5)^\circ\text{C}$ and the relative humidity was 85%. The samples were dried before placed in the box. The samples were removed and weighed at time intervals of 6, 24, 48, 72, 96, 120, 144, and 168 h. When the mass of the sample did not change between drying intervals means the moisture absorption balance was achieved. The moisture absorption rate of the composites was calculated according to the following equation:

$$c = \frac{w_1 - w_0}{w_0} \times 100\%, \quad (1)$$

where W_1 is the mass of the specimen at a certain time and W_0 is the initial mass of the specimen.

2.3.6 Thermal Conductivity

A D300FX-D15 thermal conductivity tester (Tianjin Foruide Technology Company, Tianjin, China) was used to test the thermal conductivity. The thickness of the sample plate was 8~12 mm and the transverse dimension was 100 mm \times 100 mm. Every sample was tested three times to get the average value.

3 Results and Discussion

3.1 FTIR Analysis

Fig. 3a is the FTIR spectra of bio-adhesives. The broad peak at 3,400 cm^{-1} is attributed to the –OH stretching, and the peak intensity of guar gum and chitosan was higher, which indicated that the content of –OH in guar gum and chitosan was larger than the other two bio-adhesives. The peak at 2,926 cm^{-1} is caused by the C–H stretching vibration [28]. The peak at 1,648 cm^{-1} is related to C = O, which represents the amide I group –CONH₂ in chitosan [29], and –COO– in sodium alginate [30], respectively. The peak at 1,406 cm^{-1} corresponds to the carboxylic group –COO[–] deformation vibration [31]. The peak at 1,048 cm^{-1} is associated with the C–O–H stretching [32].

Fig. 3b shows the FTIR spectra of lotus leaf fiber. The band at 2,915 cm^{-1} indicates the C–H stretching in lignin [33,34]. The peak at 1620 cm^{-1} shows the C = O groups in hemicellulose, the peaks at 1,385 and

$1,350\text{ cm}^{-1}$ are attributed to the C–H asymmetric bending vibration of the $-\text{C}(\text{CH}_3)_3$ group in lignin, the peak at $1,075\text{ cm}^{-1}$ is due to the C–O stretching of lignin [35].

Fig. 3c is the FTIR spectra comparison of the composites and bio-adhesives. The factors that enhance the bond will cause the absorption peak to move to the direction of high wavenumber, and the intensity of the absorption peak increases and widens. For each bio-adhesive and its corresponding composite, the intensity and width of the peak of the composite are larger than that of the bio-adhesive at the characteristic vibration absorption peak of hydroxyl group at $3,200\text{--}3,600\text{ cm}^{-1}$. The addition of the fibers makes the intensity of the peak increased due to they contains $-\text{OH}$, while the peak turned broader indicates that hydrogen bonds between the bio-adhesive and the fibers were formed. All the four bio-adhesives contain polar groups such as $-\text{OH}$ and $-\text{COO}^-$, which can form hydrogen bond with $-\text{OH}$ of lotus leaf fibers, which leads a certain intermolecular force between the bio-adhesives and the fibers, so that the bio-adhesives can be combined with the fibers as a whole.

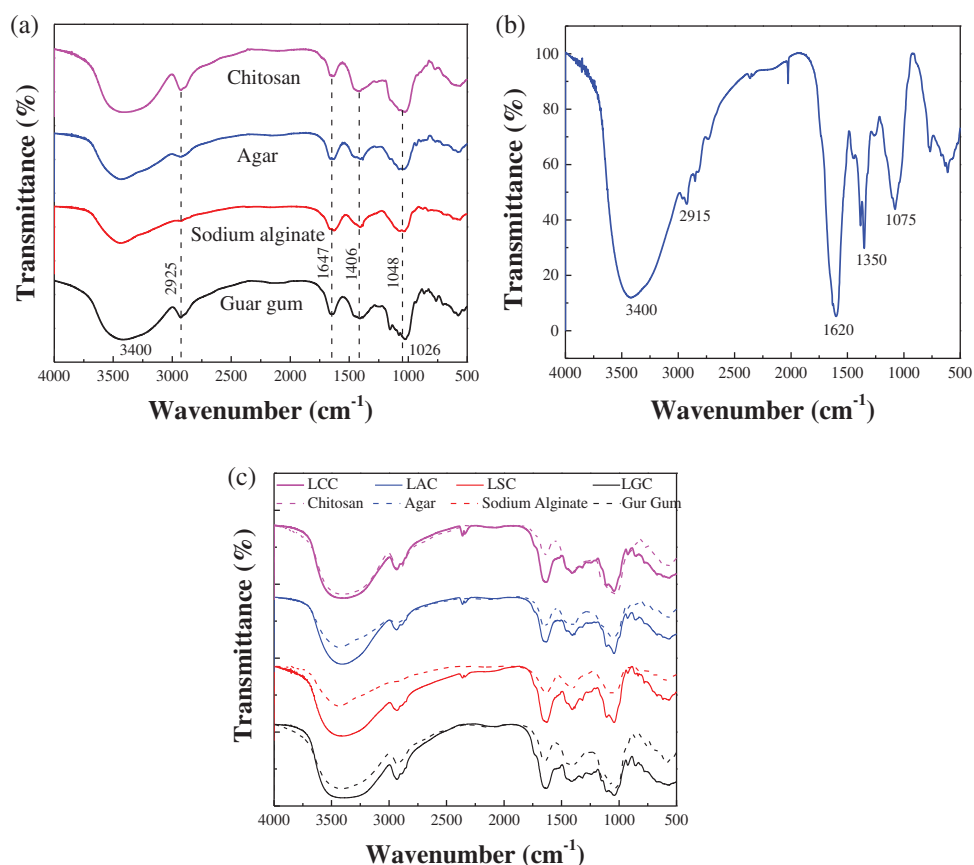


Figure 3: FTIR spectra of (a) Bio-adhesives, (b) Lotus leaf fiber and (c) The comparison of the composites and bio-adhesives

3.2 Morphology Analysis

Fig. 4 illustrates the tensile cross section of the composites. The cross section of the LAC was presented a stepped shape with few holes, the interface between agar and fibers were unobvious indicating a good combination between the two phases which was beneficial to the stress transfer of the composite. There were obvious gaps and holes in the LGC and the LSC, the interface was loose, which showed that the

combination of lotus leaf fiber with guar gum and sodium alginate was poor. In the LCC, there were many holes left by fiber pulling out and the chitosan agglomerated together, there were fewer gaps and holes compared with the LGC and the LSC. Bio-adhesive can form hydrogen bonds not only with lotus leaf fibers but also with itself. Chitosan contains different types of polar groups, which will make the formation of hydrogen bond in it more than other bio-adhesives resulting in aggregation phenomenon of chitosan, which in turn led to a poor combination between fibers.

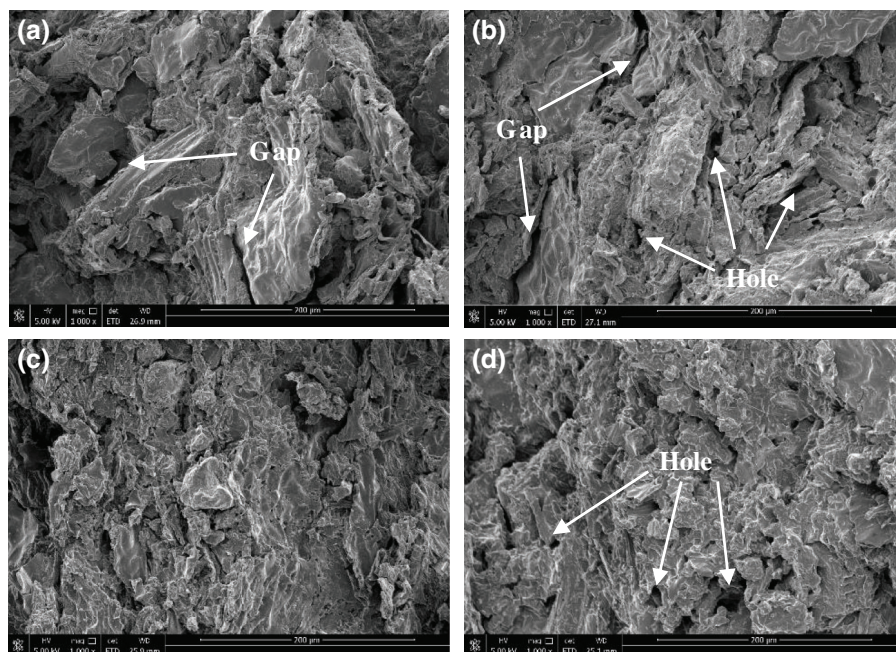


Figure 4: The tensile cross section of (a) LGC, (b) LSC, (c) LAC, and (d) LCC

3.3 Mechanical Properties

Fig. 5 shows the tensile strength, flexural strength and impact strength of the composites. The LAC had the best performance and its tensile strength, flexural strength and impact strength were 2.05 MPa, 5.9 MP and 4.29 MPa, respectively, exceeded most biomass film packaging materials [15,36]. The hydrogen bond between bio-adhesives and fibers is the main reason for their interaction, therefore, the binding effect between the two components directly affects the mechanical properties of the composites. The LAC had the best combination performance with few gaps which was beneficial to the stress transfer of the composite, so the LAC had the best mechanical properties profiles. The impact strength of the LSC and the LCC were different from those of the tensile strength and the flexural strength. The impact strength of the LSC was lower than that of other composites, while the LCC had a larger one. This may be due to the brittleness of sodium alginate compared with other bio-adhesives, which was not conducive to the consumption of energy when the composite was impacted, while the chitosan in the LCC was agglomerated, which can absorb part of the impact energy.

3.4 Thermogravimetric Analysis (TGA)

Fig. 6 is the TGA/DTG curves of the composites and the bio-adhesives. There were three major stages of thermal degradations for the composites. There was a primary mass loss in the temperature range of 60–120°C which was caused by the evaporation of the moisture in the composite. The mass loss of the LAC was the smallest, which was 4.43%, this may be related to the less internal gaps in the LAC, which

can also reduce the moisture intrusion. The second stage of decomposition was observed at the temperature ranges of 200–400°C and the cellulose components was degraded at this stage [37,38]. The initial temperature of thermal degradation of the composites decreased and the final residual rate increased after the addition of fibers, which indicates that the addition of fibers can improve the thermal stability of the composites. Among the four bio-adhesives, sodium alginate contains inorganic elements, which made the LSC have the highest residual rate and a better thermal stability.

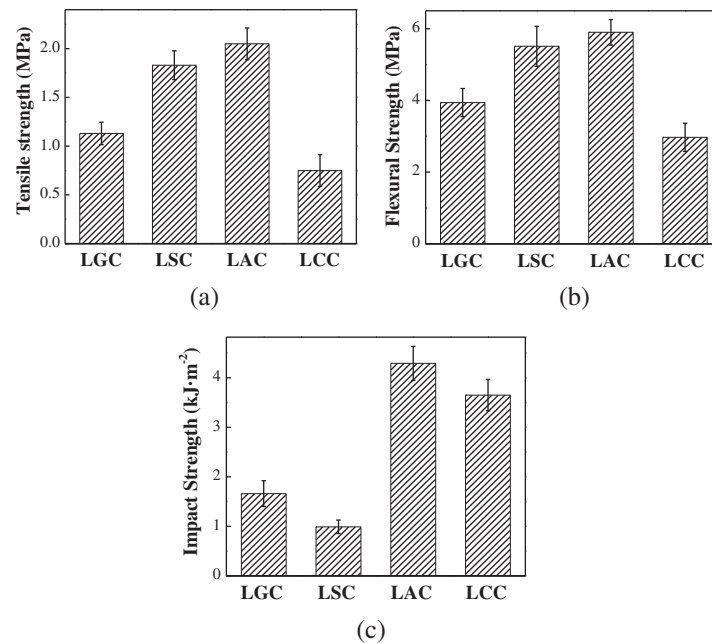


Figure 5: The (a) Tensile strength, (b) Flexural strength and (c) Impact strength of the composites

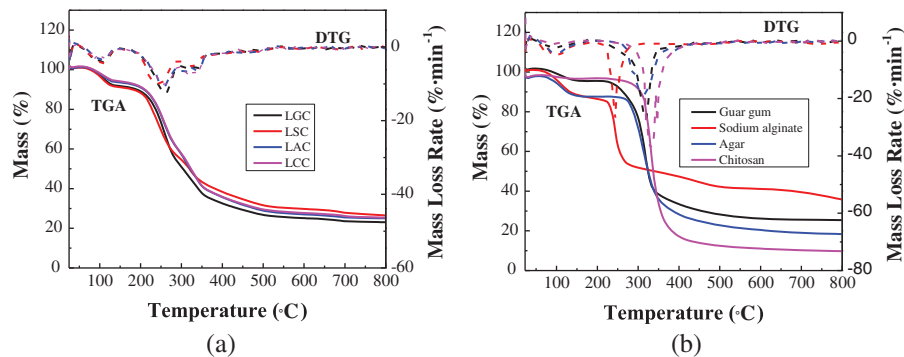


Figure 6: The TGA/DTG curves of the (a) Composites and the (b) Bio-adhesives

3.5 Moisture Absorption Performance

Fig. 7 shows the moisture absorption rate of the composites. The four composites had similar moisture absorption trend. The moisture absorption rate grew rapidly in 24 h, and then it began to slow down gradually. After 72 h, the moisture absorption rate basically remained unchanged, indicating that the composites reached the moisture absorption equilibrium. The LCC had the highest equilibrium moisture absorption rate with 39.97%. The equilibrium moisture absorption rate of the LGC and the LSC were

similar, which were 35.68% and 35.18%, respectively. The equilibrium moisture absorption rate of 32.32% of the LAC was lower than that of the other three composites, which showed that the moisture absorption performance of the LAC was lower than that of the other three composites. It can be seen that the addition of glycerin can reduce the moisture absorption of the composites to a certain extent, which may be because glycerin has plasticizing effect and prevents water molecules from entering the interior of the composites [23].

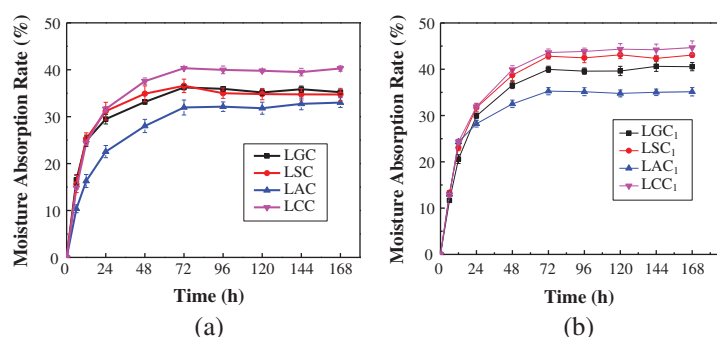


Figure 7: The moisture absorption rate of the (a) Composites and the (b) Composites without glycerin

In the composite system, both bio-adhesive and fiber contain a large number of hydrophilic groups, so they can absorb moisture. It can be seen from the FTIR spectra that the content of hydrophilic groups in chitosan and guar gum was more than other bio-adhesives, which made them a higher hygroscopicity. In addition, the combination of bio-adhesives and fibers had an important influence on the moisture absorption performance of the composites and the gaps and holes in the composites can accumulate moisture. The close combination of bio-adhesive and fiber made few gaps and hole in the composite and then reduced the moisture absorption performance. According to the cross-sectional morphology of the composite, the combination of fiber and agar is the best, and the internal gaps and holes of the composite are the least. So the LAC had the lowest moisture absorption performance and the lowest equilibrium moisture absorption rate.

3.6 Thermal Conductivity

Fig. 8 is the thermal conductivity of the composites. The LGC had the minimum thermal conductivity of $0.076 \text{ W}\cdot\text{m}^{-1}\cdot\text{k}^{-1}$, while the thermal conductivity of LSC and LAC were similar, which were 0.092 and $0.094 \text{ W}\cdot\text{m}^{-1}\cdot\text{k}^{-1}$, respectively. The internal structure of the composites had an important influence on the thermal conductivity. There were a large number of gaps and holes in the LGC which would increase its internal air content, and the excellent thermal insulation performance of air reduced its thermal conductivity. The LAC had a good internal combination and few holes, so its thermal conductivity was big. The four composites were thermal insulating materials since the thermal conductivity was less than $0.23 \text{ W}\cdot\text{m}^{-1}\cdot\text{k}^{-1}$.

3.7 Comparison of Properties of Composites

Table 1 shows the comparison of the performance between the degradable packaging materials sold on the market and the composites prepared in this paper. It can be seen that LAC has the best comprehensive properties in the bio-adhesive/lotus leaf fiber composites. The mechanical properties of LAC are lower than those of corn starch/polypropylene materials, but better than those of paper materials. The moisture absorption performance of corn starch/polypropylene is the lowest, which is mainly due to the low water absorption of polypropylene plastic. Overall, LAC can be used to substitute plastics to reduce environmental pollution in the scenario of low performance requirements but completely degradable.

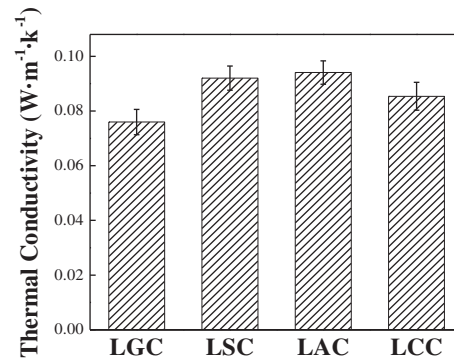


Figure 8: The thermal conductivity of the composites

Table 1: The comparison of properties of composites

Component	Origin	Tensile strength (MPa)	Flexural strength (MPa)	Impact strength (MPa)	Thermal conductivity (W·m ⁻¹ ·k ⁻¹)	Equilibrium moisture absorption rate (%)
Wheat straw paper	Market	0.67	1.76	2.56	0.013	22.62
60% Corn starch/40% Polypropylene	Market	5.46	7.28	1.24	0.035	12.45
LGC	–	1.13	3.94	1.66	0.076	35.68
LSC	–	1.83	5.51	0.99	0.092	35.18
LAC	–	2.05	5.90	4.29	0.094	32.32
LCC	–	0.75	2.97	3.65	0.085	39.97

4 Conclusions

The bio-adhesives contained polar groups such as –OH and –COO⁻, which can form hydrogen bonds with –OH in lotus leaf fibers, and can effectively promote the combination of bio-adhesives and lotus leaf fibers. The thermal conductivity of the four composites was all less than 0.23 W·m⁻¹·k⁻¹, showing that they were thermal insulating materials. The LAC had a good internal combination with few internal defects induced the best mechanical properties, and the tensile strength, flexural strength and impact strength were 2.05, 5.9 MPa and 4.29 kJ·m⁻², respectively. The good interfacial structure lead it a low moisture absorption performance, and its equilibrium moisture absorption rate was 32.32%. Overall, the LAC has the best performance, which had a feasibility to substitute plastic packaging materials in some scenarios.

Acknowledgement: This work was financially supported by the Regional Cooperative Innovation in Autonomous Region (2019E0241), China.

Funding Statement: The authors received no specific funding for this study.

Conflicts of Interest: The authors declare that they have no conflicts of interest to report regarding the present study.

References

1. Napper, I. E., Davies, B. F. R., Clifford, H., Elvin, S., Koldewey, H. J. et al. (2020). Reaching new heights in plastic pollution—preliminary findings of microplastics on Mount Everest. *One Earth*, 3(5), 621–630. DOI 10.1016/j.oneear.2020.10.020.
2. Conti, G. O., Ferrante, M., Banni, M., Favara, C., Nicolosi, I. et al. (2020). Micro- and nano-plastics in edible fruit and vegetables. The first diet risks assessment for the general population. *Environmental Research*, 187(12), 109677. DOI 10.1016/j.envres.2020.109677.
3. Abbasi, S., Soltani, N., Keshavarzi, B., Moore, F., Turner, A. et al. (2018). Microplastics in different tissues of fish and prawn from the Musa Estuary, Persian Gulf. *Chemosphere*, 205(4501), 80–87. DOI 10.1016/j.chemosphere.2018.04.076.
4. Dessi, C., Okoffo, E. D., O'Brien, J. W., Gallen, M., Samanipour, S. et al. (2021). Plastics contamination of store-bought rice. *Journal of Hazardous Materials*, 416(1–4), 125778. DOI 10.1016/j.jhazmat.2021.125778.
5. Schymanski, D., Goldbeck, C., Humpf, H. U., Fuerst, P. (2018). Analysis of microplastics in water by micro-raman spectroscopy: Release of plastic particles from different packaging into mineral water. *Water Research*, 129(4062), 154–162. DOI 10.1016/j.watres.2017.11.011.
6. Kutralam-Muniasamy, G., Perez-Guevara, F., Elizalde-Martinez, I., Shruti, V. C. (2020). Branded milks-are they immune from microplastics contamination? *Science of Total Environment*, 714(4), 136823. DOI 10.1016/j.scitotenv.2020.136823.
7. Manfra, L., Marengo, V., Libralato, G., Costantini, M., de Falco, F. et al. (2021). Biodegradable polymers: A real opportunity to solve marine plastic pollution? *Journal of Hazardous Materials*, 416(10), 125763. DOI 10.1016/j.jhazmat.2021.125763.
8. Charitou, A., Aga-Spyridopoulou, R., Mylona, N., Beck, Z., McLellan, Z. et al. (2021). Investigating the knowledge and attitude of the Greek public towards marine plastic pollution and the EU single-use plastics directive. *Marine Pollution Bulletin*, 166, 112182. DOI 10.1016/j.marpolbul.2021.112182.
9. Willis, K. A., Hardesty, B. D., Wilcox, C. (2021). State and local pressures drive plastic pollution compliance strategies. *Journal of Environmental Management*, 287, 112281. DOI 10.1016/j.jenvman.2021.112281.
10. Chowdhury, G. W., Koldewey, H. J., Duncan, E., Napper, I. E., Niloy, M. N. H. et al. (2021). Plastic pollution in aquatic systems in Bangladesh: A review of current knowledge. *Science of Total Environment*, 761, 143285. DOI 10.1016/j.scitotenv.2020.143285.
11. Li, C., Sun, M., Xu, X., Zhang, L., Guo, J. et al. (2021). Environmental village regulations matter: Mulch film recycling in rural China. *Journal of Cleaner Production*, 299(2), 126796. DOI 10.1016/j.jclepro.2021.126796.
12. Li, M., Tian, X., Jin, R. F., Li, D. (2018). Preparation and characterization of nanocomposite films containing starch and cellulose nanofibers. *Industrial Crops and Products*, 123(10), 654–660. DOI 10.1016/j.indcrop.2018.07.043.
13. Ramesh, S., Radhakrishnan, P. (2019). Cellulose nanoparticles from agro-industrial waste for the development of active packaging. *Applied Surface Science*, 484(1), 1274–1281. DOI 10.1016/j.apsusc.2019.04.003.
14. Ortega-Toro, R., Contreras, J., Talens, P., Chiralt, A. (2015). Physical and structural properties and thermal behaviour of starch-poly (ϵ -caprolactone) blend films for food packaging. *Food Packaging and Shelf Life*, 5(2), 10–20. DOI 10.1016/j.fpsl.2015.04.001.
15. Li, F. Y., Guan, K. K., Liu, P., Li, G., Li, J., F. (2014). Ingredient of biomass packaging material and compare study on cushion properties. *International Journal of Polymer Science*, 2014(10), 146509. DOI 10.1155/2014/146509.
16. Jancikova, S., Jamrůz, E., Kulawik, P., Tkaczewska, J., Dordevic, D. (2019). Furcellaran/gelatin hydrolysate/rosemary extract composite films as active and intelligent packaging materials. *International Journal of Biological Macromolecules*, 131(1), 19–28. DOI 10.1016/j.ijbiomac.2019.03.050.
17. Tongdeesoontorn, W., Mauer, L. J., Wongruong, S., Sriburi, P., Reungsang, A. et al. (2021). Antioxidant films from cassava starch/gelatin biocomposite fortified with quercetin and TBHQ and their applications in food models. *Polymers*, 13(7), 1117. DOI 10.3390/polym13071117.
18. Liu, F., Chang, W., Chen, M., Xu, F., Ma, J. et al. (2020). Film-forming properties of guar gum, tara gum and locust bean gum. *Food Hydrocolloids*, 98, 105007. DOI 10.1016/j.foodhyd.2019.03.028.

19. Tavassoli-Kafrani, E., Shekarchizadeh, H., Masoudpour-Behabadi, M. (2016). Development of edible films and coatings from alginates and carrageenans. *Carbohydrate Polymers*, 137(2), 360–374. DOI 10.1016/j.carbpol.2015.10.074.
20. Mostafavi, F. S., Zaeim, D. (2020). Agar-based edible films for food packaging applications—A review. *International Journal of Biological Macromolecules*, 159(2), 1165–1176. DOI 10.1016/j.ijbiomac.2020.05.123.
21. Sun, L. J., Sun, J. J., Liu, D. J., Fu, M., Yang, X. et al. (2018). The preservative effects of chitosan film incorporated with thinned young apple polyphenols on the quality of grass carp (*Ctenopharyngodon idellus*) fillets during cold storage: Correlation between the preservative effects and the active properties of the film. *Food Packaging and Shelf Life*, 17(4), 1–10. DOI 10.1016/j.fpsl.2018.04.006.
22. Jiang, D. M., An, P. H., Cui, S. P., Xu, F., Tuo, T. et al. (2018). Effect of leaf modification methods on mechanical and heat-insulating properties of leaf fiber cement-based composite materials. *Journal of Building Engineering*, 19(10), 573–583. DOI 10.1016/j.job.2018.05.028.
23. Wang, M., He, C. X., Chang, X. N., Liu, D. N. (2016). Comparison on properties of composites prepared by four kinds of biological glues and wheat straw. *Acta Materiae Compositae Sinica*, 11(11), 2625–2633. DOI 10.13801/j.cnki.fhclxb.20160107.007.
24. GB/T 1040.1-2006 (2006). Plastics—Determination of Tensile Properties. Beijing, China: Standardization Administration of China.
25. GB/T 9341-2008 (2008). Plastics—Determination of Flexural Properties. Beijing, China: Standardization Administration of China.
26. GB/T 1043.1-2008 (2008). Plastic—Determination of Charpy Impact Properties. Beijing, China: Standardization Administration of China.
27. GB/T 20312-2006 (2006). Building Materials and Products—Determination of Damp Heat and Hygroscopic Performance. Beijing, China: Standardization Administration of China.
28. Wang, Y., Wu, J. Q., Wan, Q., Zhang, L., Lei, H. N. (2020). Preparation of chitosan/polyvinyl alcohol electrospinning nano-membranes using the green solvent, plasma acid. *Journal of Macromolecular Science, Part B*, 59(11), 731–746. DOI 10.1080/00222348.2020.1800921.
29. Karthikeyan, C., Varaprasad, K., Venugopal, S. K., Shakila, S., Venkatraman, B. R. et al. (2021). Biocidal (bacterial and cancer cells) activities of chitosan/CuO nanomaterial, synthesized via a green process. *Carbohydrate Polymers*, 529(1), 117762. DOI 10.1016/j.carbpol.2021.117762.
30. Seeli, D. S., Dhivya, S., Selyamurugan, N., Prabakaran, M. (2016). Guar gum succinate-sodium alginate beads as a pH-sensitive carrier for colon-specific drug delivery. *International Journal of Biological Macromolecules*, 91(2), 45–50. DOI 10.1016/j.ijbiomac.2016.05.057.
31. Daud, H., Ghani, A., Iqbal, D. N., Ahmad, N., Nazir, S. et al. (2021). Preparation and characterization of guar gum based biopolymeric hydrogels for controlled release of antihypertensive drug. *Arabian Journal of Chemistry*, 14(5), 103111. DOI 10.1016/j.arabjc.2021.103111.
32. Dai, F. F., Yu, J., Yuan, M. Q., Deng, Z. M., Wang, Y. Q. et al. (2021). Enhanced cellular compatibility of chitosan/collagen multilayers LBL modified nanofibrous mats. *Materials & Design*, 205(1), 109717. DOI 10.1016/j.matdes.2021.109717.
33. Krishnaiah, P., Ratnam, C. T., Manickam, S. (2017). Enhancements in crystallinity, thermal stability, tensile modulus and strength of sisal fibres and their PP composites induced by the synergistic effects of alkali and high intensity ultrasound (HIU) treatments. *Ultrasonics Sonochemistry*, 34, 729–742. DOI 10.1016/j.ultsonch.2016.07.008.
34. Oure, A., Jauregi, A., Pena-Rodriguez, C., Labidi, J., Eceiza, A. et al. (2015). The effect of surface modifications on sisal fiber properties and sisal/poly (lactic acid) interface adhesion. *Composites Part B: Engineering*, 73(3), 132–138. DOI 10.1016/j.compositesb.2014.12.022.
35. Senthilkumar, K., Rajini, N., Saba, N., Chandrasekar, M., Jawaid, M. et al. (2019). Effect of alkali treatment on mechanical and morphological properties of pineapple leaf fibre/polyester composites. *Journal of Polymers and the Environment*, 27(6), 1191–1201. DOI 10.1007/s10924-019-01418-x.
36. Ghoshal, G., Singh, D. (2020). Synthesis and characterization of starch nanocellulosic films incorporated with eucalyptus globulus leaf extract. *International Journal of Food Microbiology*, 332(4), 108765. DOI 10.1016/j.ijfoodmicro.2020.108765.

37. Santos, V. T. D., Siqueira, G., Miagres, A. M. F., Ferraz, A. (2018). Role of hemicellulose removal during dilute acid pretreatment on the cellulose accessibility and enzymatic hydrolysis of compositionally diverse sugarcane hybrids. *Industrial Crops and Products*, 111, 722–730. DOI 10.1016/j.indcrop.2017.11.053.
38. Wang, L. Y., Dong, Y., Men, H. T., Tong, J., Zhou, J. (2013). Preparation and characterization of active films based on chitosan incorporated tea polyphenols. *Food Hydrocolloids*, 32(1), 35–41. DOI 10.1016/j.foodhyd.2012.11.034.